Molecular Biology Reports (2021) 48:5473–5484
https://doi.org/10.1007/s11033-021-06557-w

ORIGINAL ARTICLE

Exosomes derived from astrocytes after oxygen-glucose deprivation promote differentiation and migration of oligodendrocyte precursor cells in vitro

Yaping Xu[1,2] · Yeye Tian[1] · Yao Wang[1] · Li Xu[1] · Guini Song[1] · Qiao Wu[1] · Wei Wang[1,3] · Minjie Xie[1,3]

Received: 22 October 2020 / Accepted: 9 July 2021 / Published online: 26 July 2021

Abstract

Background Excessive release of glutamate, oxidative stress, inflammation after ischemic brain injury can lead to demyelination. Astrocytes participate in the maturation and differentiation of oligodendrocyte precursor cells (OPCs), and play multiple roles in the process of demyelination and remyelination. Here, we studied the role of Astrocyte-derived exosomes (AS-Exo) under ischemic conditions in proliferation, differentiation and migration of OPCs in vitro.

Methods and results Exosomes were collected from astrocytes supernatant by differential centrifugation from control astrocytes (CT^{exo}), mild hypoxia astrocytes ($O2R24^{exo}$) which were applied oxygen-glucose deprivation for 2 h and reperfusion for 24 h (OGD2hR24h) and severe hypoxia astrocytes ($O4R24^{exo}$) which were applied oxygen-glucose deprivation for 4 h and reperfusion for 24 h (OGD4hR24h). Exosomes (20 μg/ml) were co-cultured with OPCs for 24 h and their proliferation, differentiation and migration were detected. The results showed that AS-Exo under severe hypoxia ($O4R24^{exo}$) inhibit the proliferation of OPCs. Meanwhile, all exosomes from three groups can promote OPCs differentiation and migration. Compared to control, the expressions of MAG and MBP, markers of mature oligodendrocytes, were significantly increased in AS-Exo treatment groups. AS-Exo treatment significantly increased chemotaxis for OPCs.

Conclusions AS-Exo improve OPCs' differentiation and migration, whereas AS-Exo with severe hypoxic precondition suppress OPCs' proliferation. AS-Exo may be a potential therapeutic target for myelin regeneration and repair in white matter injury or other demyelination related diseases.

Keywords Astrocyte-derived exosomes · Oxygen-glucose deprivation · Oligodendrocyte precursor cells · Proliferation · Differentiation · Migration

Introduction

Excessive release of glutamate, oxidative stress and inflammation after ischemic brain injury can lead to demyelination [1, 2]. Astrocytes participate in the maturation and differentiation of oligodendrocyte precursor cells (OPCs), and play multiple roles in the process of demyelination and remyelination. Astrocytes can provide nutritional and metabolic support to other neural cells of the central nervous system (CNS) [3, 4], playing a vital role in modulating of CNS extracellular environment in which oligodendrocyte precursor cells (OPCs) settle. They have many important and complex functions that can directly affect the generation and survival of oligodendrocyte lineage cells [3]. Various cytokines secreted by astrocytes are closely related to myelin injury and regeneration. We previously have showed that inhibition of Cx43 gap junction channel in astrocytes

✉ Minjie Xie
xie_minjie@126.com

1 Department of Neurology, Tongji Hospital, Tongji Medical College, Huazhong University of Science and Technology, No. 1095 Jiefang Avenue, Wuhan 430030, People's Republic of China

2 Department of Neurology, Xiangyang No. 1 People's Hospital, Hubei University of Medicine, Xiangyang 441000, People's Republic of China

3 Key Laboratory of Neurological Diseases of Chinese Ministry of Education, The School of Basic Medicine, Tongji Medical College, Huazhong University of Science and Technology, Wuhan 430030, People's Republic of China

under hypoxia can promote the differentiation of OPCs into mature oligodendrocytes [5]. However, the specific role and the underlying mechanism of astrocytes in myelin injury and regeneration remains to be further explored.

Exosomes are nano-sized membrane vesicles with a lipid bilayer structure secreted by almost all living cells, which contain cell-specific proteins, lipids, and nucleic acids (mRNA, miRNA, LncRNA), and the diameter is between 30 and 150 nm [6–8]. They have the ability to cross the blood–brain barrier and play an important role in cell communication between neurons and glial cells [7]. Studies indicate that Astrocyte-derived exosomes (AS-Exo) are actively involved in the pathological process of stroke, traumatic brain injury and other neurological diseases [9, 10]. AS-Exo inhibit autophagy by mediating the transfer of miR-190b reducing neuronal damage in experimental ischemic stroke [11, 12]. The secretion of microvesicles containing Aβ can induce apoptosis of cortical neurons, which plays an important role in the progression of Alzheimer's disease [13]. The level of IL-6 in AS-Exo of ALS patients is elevated, and positively correlated with the rate of disease progression [14]. However, the role of AS-Exo in myelin regeneration and repair in white matter injury needs to be explored.

In this study, we established a simulated ischemia model to study the effects of AS-Exo on oligodendrocytes precursor cells' proliferation, differentiation and migration in vitro. The results showed that AS-Exo in hypoxia conditions promoted the differentiation and migration of oligodendrocyte precursor cells whereas AS-Exo from severe hypoxia condition inhibited the proliferation of OPCs. AS-Exo might provide a potential therapeutic target in remyelination.

Materials and methods

Astrocyte and OPCs culture

All animal procedures were approved by the Institutional Animal Care and Use Committee of the Huazhong University of Science and Technology. Rat Sprague–Dawley pups (P0–P2) were obtained from the Experimental Animal Center of Tongji Medical College, Huazhong University of Science and Technology. The culture of mixed glial cells was prepared as previously described [15–17] with minor modifications. Briefly, cerebral tissue was extracted from rat Sprague–Dawley pups (P0–P2). After removed the meninges, it was cut into small pieces and digested with 0.25% trypsin (Genom, China). Cells were cultured with Dulbecco's Modified Eagle's Medium and Ham's F12 (DMEM/F12, Hyclone, USA) plus 1% penicillin/streptomycin with 10% fetal bovine serum (FBS, sijiqing, China) and plated on 75-cm^2 flasks coated with poly-D-lysine (Sigma-Aldrich, USA). The cell medium was changed every 2 days with 10% FBS in DMEM/high glucose (Hyclone, USA). Cultures were incubated at 37 °C and 5% CO_2.

For isolation of OPCs, microglia were removed by shaking for 2 h at 200 rpm at 37°C. Then, the cell supernatant containing OPCs was obtained after shaking for 18 h at 220 rpm, filtered through a filter with an aperture of 40 μm and preplated on a 100 mm uncoated sterile Petri dish for 1 h. Purified OPCs were seeded onto poly-D-lysine coated glass coverslips or plates, and maintained in medium consisting of DMEM/F12 (Hyclone, USA) supplemented with 1% N2 (Gibco, USA), 1% B27 (Gibco, USA), 10 ng/ml PDGF-AA (Peprotech, USA), 10ng/ml FGF-basic (Peprotech, USA) to promote proliferation (proliferation medium). After 1 day in culture, platelet-derived growth factor receptor α^+ (PDGFRα^+) OPCs accounted for 95%. And differentiated culture was performed 2 days later in medium of DMEM/F12 (Hyclone, USA) supplemented with 1% N2 (Gibco, USA), 1% B27 (Gibco, USA), 10 ng/ml CNTF (Peprotech, USA), 50 ng/ml T3 (Invitrogen, USA) to allow differentiation (differentiation medium).

After microglia and OPCs removal, trypsin was added for digestion and then the supernatant was collected for centrifugation. Purified astrocytes were plated onto poly-D-lysine coated coverslips in 24-well culture dishes at a density of 4×10^4 cells/well or six-well plates at a density of 4×10^5 cells/well. In purified cultures, more than 95% cells were glia fibrillary acidic protein-positive ($GFAP^+$).

Exosome-free FBS

Exosomes in fetal bovine serum were removed by filtration and ultracentrifugation. First, a 0.22 μm needle filter was used to filter FBS, then FBS was transferred to an ultracentrifuge tube and centrifuged at a speed of 150,000×*g* for 7 h. Finally, we collected the supernatant in tube and discarded the precipitate to obtain exosome-free FBS.

Oxygen-glucose deprivation

Oxygen-glucose deprivation (OGD) was performed as previously described [15, 17]. Astrocytes were incubated in DMEM/F12 supplemented with 10% FBS, and medium was changed every 2 days. Monolayer astrocytes were tiled to 80–90% of the petri dish for further processing, washed twice and incubated in glucose-free DMEM (Gibco, USA). Then, astrocytes were transferred into anoxic incubator with a gas mixture of 92% N_2/5% CO_2/3% O_2 at 37 °C. Fresh medium (DMEM/F12 supplement with 5% exo-free FBS) was replaced for reperfusion culture for 24 h after 2 h and 4 h of hypoxia. As normal control, astrocytes were cultured in medium (DMEM/F12 supplement with 5% exo-free FBS) with normoxic and maintained in standard incubation

conditions. The cell supernatants from all groups were collected for further study after 24 h reperfusion.

Exosomes' isolation and characterization

Exosomes were isolated from the cell culture supernatant of astrocyte in control (CT^{exo}) (n = 37), OGD2hR24h ($O2R24^{exo}$) (n = 39), and OGD4hR24h ($O4R24^{exo}$) (n = 39). The culture supernatant was collected after 24 h reperfusion and went through sequential ultracentrifugation at 300×*g* for 10 min to remove living cells, 2000×*g* for 10 min to remove dead cells, 12,000×*g* for 30 min to remove cell debris, 120,000×*g* for 3 h to get exosomes at 4 °C. The exosomes were washed once with phosphate-buffered saline (PBS) at 120,000×*g* for 100 min and suspended with 100 µl PBS.

A transmission electron microscopy (JEM-1200EX, Japan) was used to identify the morphology of exosomes. The exosomes (10 µl) were loaded on the copper electron microscope grid for 3 min, and marked with phosphotungstic acid solution, dried at room temperature for 5 min, and then imaged on the machine. Exosomal protein markers (CD63 and Alix) and albumin were detected by western blot. All samples were measured using nanoparticle tracking analysis (NTA) with Zeta View S/N 17–310 (Germany) and corresponding software Zeta View 8.04.02.

Exosomes labeling and uptake

Exosomes were labeled with a PKH26 fluorescent labeling kit (Sigma, USA) according to the instructions. Briefly, exosome samples were added 1 ml Diluent C from the PKH26 kit, and then added 5 µl PKH26 dye into the 1 ml Diluent C tubes, mixed continuously for 30 s by gentle pipetting. Quenched reaction was induced by adding 2 ml 10% BSA in PBS for 5 min at room temperature. Then 1.5 ml of a 0.971 M sucrose solution was added by pipetting slowly and carefully into the bottom of tube. The exosome pellet was resuspended in PBS by gentle pipetting after centrifuging at 120,000×*g* for 3 h at 4 °C. Subsequently, OPCs were incubated with the PKH26-labeled exosomes for 24 h. The cells were fixed and stained with 4,6-diamidino-2-phenylindole (DAPI), and images were taken under a confocal microscope (Olympus, FV500, Japan).

Cell Counting Kit-8

For Cell Counting Kit-8 (CCK-8; Dojindo, Japan) assay, astrocytes were cultured on 96-well plates at a density of 5000 cells/well. Astrocytes' viability was detected by a CCK-8 assay after oxygen-glucose deprivation treatment at different time according to manufacturer's methods.

Immunofluorescence staining

The cells were fixed with ice cold 4% paraformaldehyde for 15 min, permeabilized with 0.25% Triton X-100 in PBS, blocked with 10% bovine serum albumin (BSA) for 1 h at room temperature, then incubated with primary antibodies (rabbit anti-glia fibrillary acidic protein [GFAP] [1:200; Cell Signaling technology, USA], anti-rabbit PDGFR-α [1:200; Abcam, Cambridge], rat anti-myelin basic protein [MBP] [1:200; Millipore, USA], mouse anti-myelin-associated glycoprotein [MAG] [1:200; Santa Cruz Biotechnology, USA] with 5% BSA overnight at 4 °C, and incubated for 1 h at room temperature with the appropriate secondary antibody (fluorescein isothiocyanate [FITC]-conjugated goat anti-mouse IgG, Alexa Fluor 594-conjugated goat anti-rat IgG, cyanine3-conjugated goat anti-rabbit IgG, Alexa Fluor 488-conjugated goat anti-Rabbit IgG [1:200; Jackson-ImmunoResearch]). The images were captured using a fluorescent microscope (Olympus, BX51, Japan) and laser confocal microscope (Olympus, FV5000, Japan). Cells were counted in visual field by Image J software.

OPCs proliferation assay

OPCs were exposed to AS-Exo (20 µg/ml) for 24 h in proliferation medium after OPCs purification on glass coverslips for 1 day. 5-Ethynyl-2-deoxyuridine (EdU) was detected by the Cell-Light™ EdU Apollo® 567 In Vitro Imaging Kit (Ribobio) following the manufacturer's instructions. Then, coverslips were incubated with DAPI to reveal total nuclei. Images of the stained coverslips were acquired with a fluorescence microscope (Olympus, BX51). EdU-DAPI double positive cells were counted by ImageJ cell counter plugin. The protein was extracted from each group. The expression of PDGFR-α was detected by western blot.

OPCs differentiation assay

OPCs were cultured for 2 days in proliferation medium, and then shifted into differentiation medium with AS-Exo (20 µg/ml) for 24 h. Cells were fixed with 4% paraformaldehyde and stained with anti-myelin basic protein (MBP), anti-myelin-associated glycoprotein (MAG) to detect cell differentiation. MBP and MAG-positive cells were counted by ImageJ. In statistical analysis, we calculated the expression levels of MBP+ and MAG+ cells and the total number of cells in each field. The cells protein was extracted from each group. The expression of MBP and MAG, the protein marker in mature oligodendrocytes, was detected by western blot.

OPCs migration assay

Migration of OPCs were performed in chambers (5 μm pore size filter; Constar, Corning, USA) as previously described [18, 19]. Briefly, the upper chamber was seeded with 5×10^4 OPCs in 200 μl of DMEM/F12, and the lower chamber was filled with 600 μl of DMEM/F12 (negative control), proliferation medium (positive control), and exosomes from different groups of astrocytes in DMEM/F12. After 24 h of incubation at 37 °C with 5% CO_2, non-migrated cells were removed from the upper surface of the filter with a cotton swab, whereas migrated cells in the lower side of the filter were fixed with 4% paraformaldehyde (PFA) for 15 min and stained with 1% crystal violet for 30 min. The number of migrated cells were determined by 8–10 random fields per well, and counted using ImageJ cell counter plugin. All experiments were run at least triplicate for each group.

Western blot

Total proteins were collected from cells samples using RIPA lysis buffer (Beyotime, Haimen, China) with protease inhibitor cocktail and quantified with the BCA kit (Beyotime Biotechnology, Haimen, Jiangsu Province, China). The proteins were subsequently transferred to a nitrocellulose membrane (0.45 μm, Millipore, USA) after sodium dodecyl sulfate polyacrylamide gel electrophoresis (SDS-PAGE). Then, the membranes were blocked in 5% non-fat milk for 1 h at room temperature. The membranes were incubated with primary antibodies of mouse anti-CD63 (1:1000, Santa Cruz biotechnology, USA), Rabbit anti-Albumin (1:1000, Proteintech, USA), mouse anti-Alix (1:1000, Cell Signaling technology, USA), rabbit anti-PDGFR-α (1:1000, Abcam, Cambridge), rat anti-MBP (1:1000, Millipore, USA), mouse anti-MAG (1:1000, Santa Cruz Biotechnology, USA), rabbit anti-β-actin (1:1000, servicebio, China) at 4 °C overnight. After washing three times with Tris-buffered saline containing 0.1% Tween-20 (TBST), the membranes were incubated with the HRP-conjugated secondary antibody (goat anti-rabbit IgG, goat anti-rat IgG, goat anti-mouse IgG, 1:5000, Promoter, China) for 1 h at room temperature. The protein bands were visualized with Bio-Rad ChemiDoc XRS+ imaging system. Photographic development was by chemiluminescence (ECL, servicebio, China). And intensity of each band was analyzed by ImageJ. The expression level of each protein was normalized to β-actin.

Statistical analysis

All experimental data from at least three independent experiments analyzed by GraphPad Prism 6.0 software (GraphPad Software, USA). The results were presented as mean ± standard deviation (SD). Statistical comparisons were realized with one-way analysis of variance (ANOVA) for multiple comparisons between groups. Differences between groups were considered statistically significant when P value < 0.05.

Results

Effects of oxygen-glucose deprivation and reperfusion (OGD/R) on astrocyte activation

Purified astrocytes were identified by immunostaining with GFAP. And $GFAP^+$ cells reached 95% after 2 days culture (Fig. 1a). After astrocytes exposure to normoxia or OGD/R, the CCK8 assay was used to assess the viability of astrocytes. We tested four durations of OGD, which were 0.5 h, 1 h, 2 and 4 h, respectively. At acute phase (0 h reperfusion), cell survival rate decreased significantly after OGD for 4 h (Fig. 1b). However, cell survival rate increased significantly after astrocytes were deprived of oxygen and glucose for 2 h and reperfusion for 24 h, which was possibly due to proliferation (Fig. 1c). GFAP immunofluorescence staining at OGD2hR24h and OGD4hR24h was used to verify the activation of astrocytes. The results showed that astrocytes in control group presented a flat and polygonal morphology. In OGD2hR24h and OGD4hR24h groups, astrocytes became hypertrophy and clustered (Fig. 1d). Quantitative analysis results showed that GFAP fluorescence intensity (the average fluorescence intensity of single cell) increased in group of OGD2hR24h and OGD4hR24h (Fig. 1e).

Isolation, identification and uptake of exosomes

Exosomes were collected from astrocytes' supernatant by sequential ultracentrifugation (Fig. 2a). Three experimental groups of AS-Exo were used in the following experiments: control exosomes (CT^{exo}), OGD2hR24 exosomes ($O2R24^{exo}$), OGD4hR24 exosomes ($O4R24^{exo}$). The typical cup-like membrane vesicle morphology was observed by transmission electron microscopy (Fig. 2b). Western blot analysis showed that exosome markers including Alix and CD63 were expressed in exosomes of all three groups. Albumin was a common pollutant in exosomes, and it was barely expressed in each group (Fig. 2c). Nanoparticle tracking analysis (NTA) indicated that exosomes had a narrow size distribution, and the peaks of exosomal dimeters were located at 117.5 nm, 133.3 nm and 113.5 nm, respectively (Fig. 2d).

The expression of PDGFR-α (a marker of OPCs) was detected by immunofluorescence, and PDGFR-α^+ cells reached 95% after OPCs were cultured in proliferation medium for one day (Fig. S1). Exosomes were labeled with a PKH26 fluorescent labeling which can mark the cell

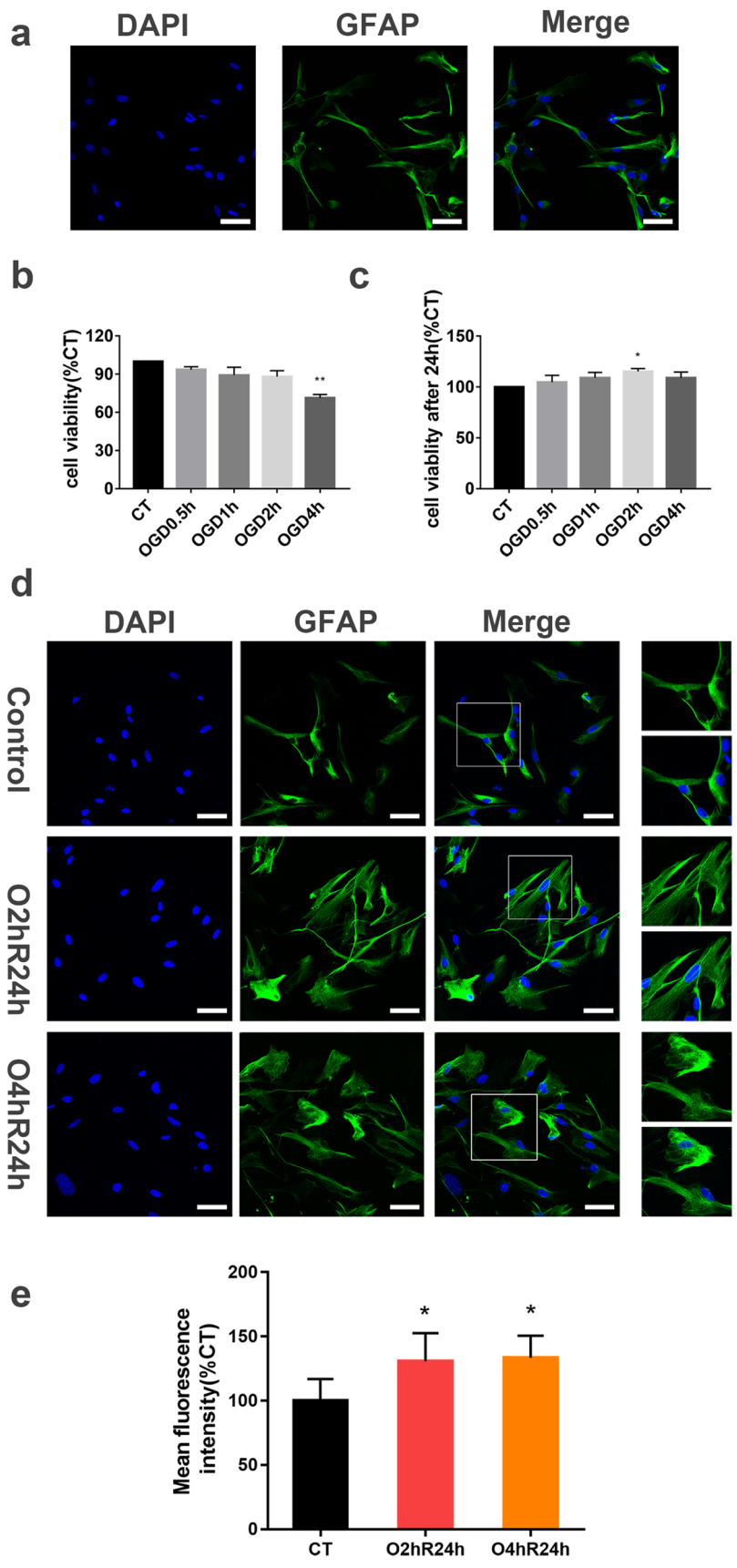

Fig. 1 Effects of OGD duration on cell viability of astrocytes. **a** Astrocytes were identified by GFAP immunofluorescence staining. Scale bar = 50 μm. **b**, **c** Cell viability of astrocytes exposed to OGD for 0.5 h, 1 h, 2 h, 4 h, followed by reperfusion for 24 h. **d** GFAP immunostaining after OGD2hR24h, OGD4hR24h and control. Scale bar = 50 μm. **e**. Statistical results of GFAP in mean fluorescence intensity. Values are from 4 independent experiments. *p < 0.05; **p < 0.01; ***p < 0.001

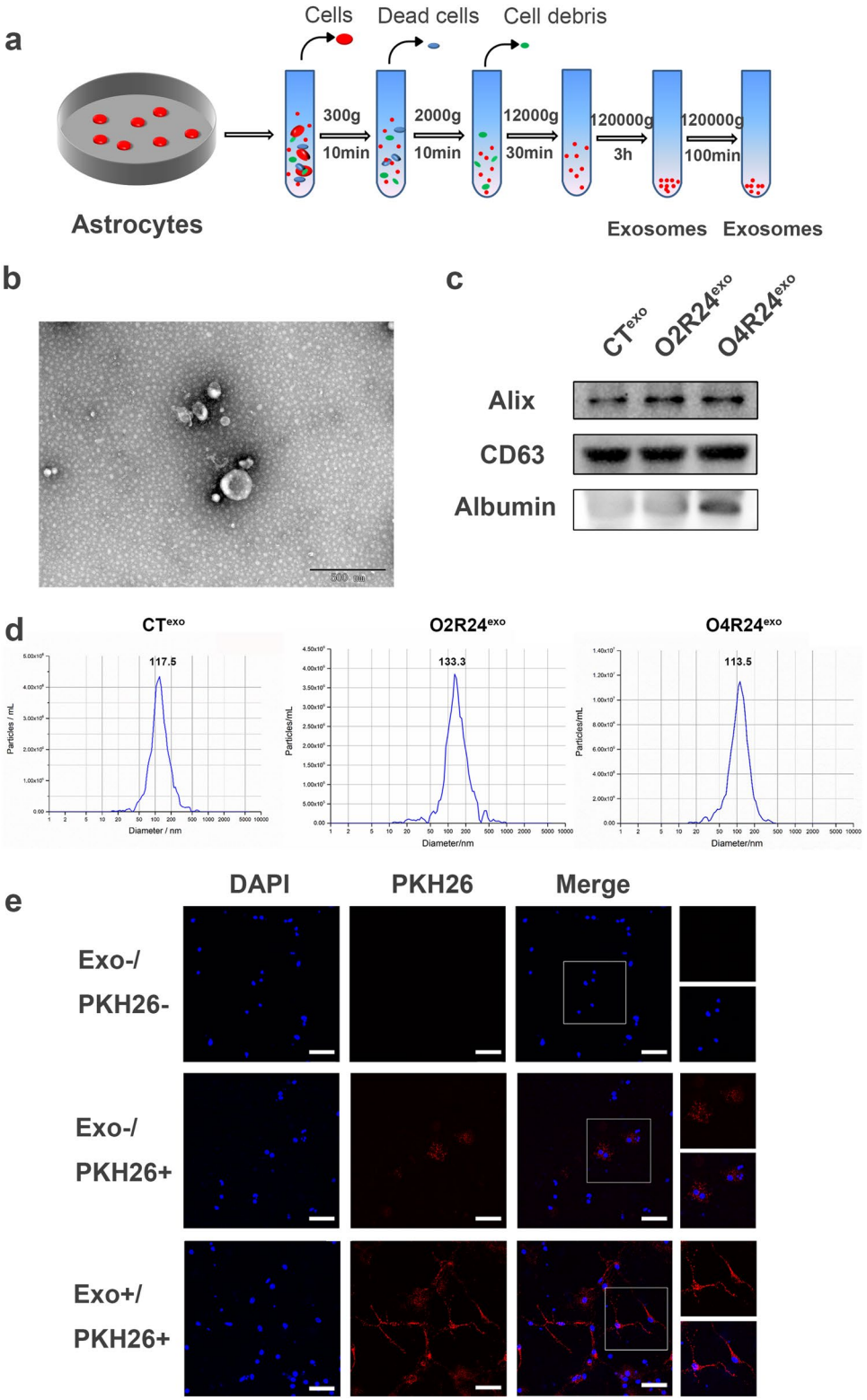

Fig. 2 Isolation, identification and uptake of exosomes. **a** Schematic diagram of exosomes preparation: astrocytes' supernatant was collected after OGD2hR24h, OGD4hR24h and control, then differential centrifugation was performed to obtain pure exosomes. **b** The morphology of exosomes was examined by transmission electron microscopy. Scale bar = 500 nm. **c** Exosomal protein markers (CD63 and Alix) and albumin were detected by western blot. **d** Particle size by nanoparticle tracking analysis for AS-Exos. **e** The nuclei had nothing around without exosomes in control. AS-Exo labeled by PKH26 (red) enter the cytoplasm of OPCs and surround nuclei. The nuclei were labeled with DAPI. Scale bar = 50 μm

membrane structure, so exosomes can be well traced. OPCs were incubated with exosomes in order to examine their uptake by these cells. Confocal images showed that PKH26-labeled exosomes (red) were localized in the cytoplasm and outline the shape of the OPCs, indicating exosomes were taken up by OPCs. A PKH26 negative control experiment showed that a small amount of dye entered the OPCs and no dye signal was observed in the blank control group (Fig. 2e).

Astrocyte-derived exosomes inhibit the proliferation of OPCs under severe hypoxia condition

After 1 day of OPCs culture, the medium was replaced with proliferation medium containing exosomes (CT^{exo}, $O2R24^{exo}$, $O4R24^{exo}$, 20 μg/ml) or PBS using the same volume as control for 24 h (Fig. 3a). We examined the effect of exosomes on proliferation of OPCs by measuring EdU staining and western blot. A significant decrease in the percentage of EdU out of DAPI cells was observed with $O4R24^{exo}$ as compared to control and CT^{exo}, whereas those

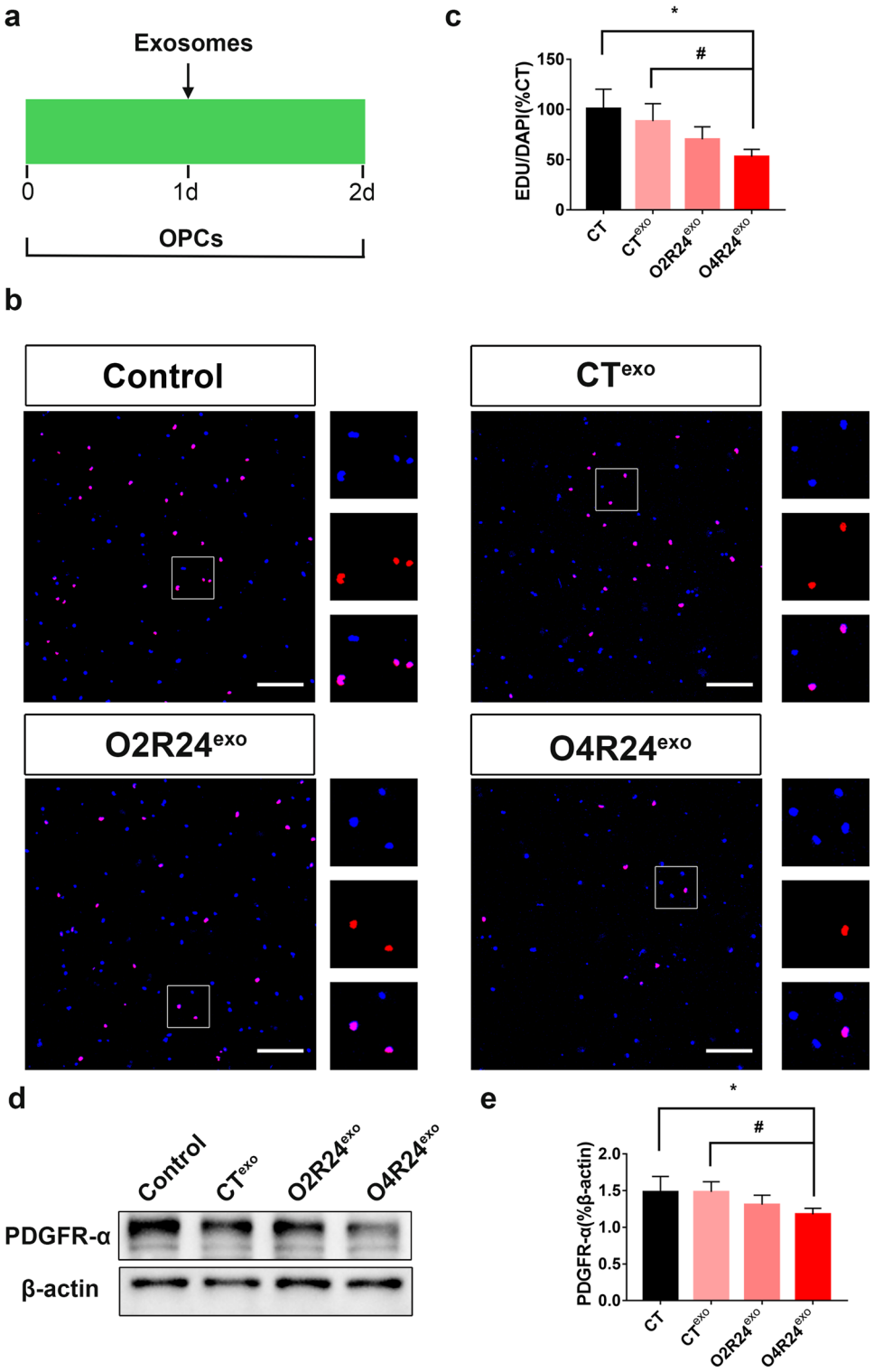

Fig. 3 Effects of exosomes derived from astrocytes after oxygen-glucose deprivation on the proliferation of OPCs. **a** Schematic diagram of the co-culture process of OPCs and AS-Exo in proliferation. **b** Representative images of EdU and DAPI staining of OPCs in 4 groups. Scale bar = 100 μm. **c** Statistical results of the percentage of EdU positive cells in OPCs culture after AS-Exo treatment. **d** Representative images of western blot for PDGFR-α and β-actin in OPCs after control and AS-Exo treatment. **e** Quantitative analysis of the expression of PDGFR-α in OPCs after control and AS-Exo treatment normalized to β-actin. Data are presented as mean ± SD (n = 4)

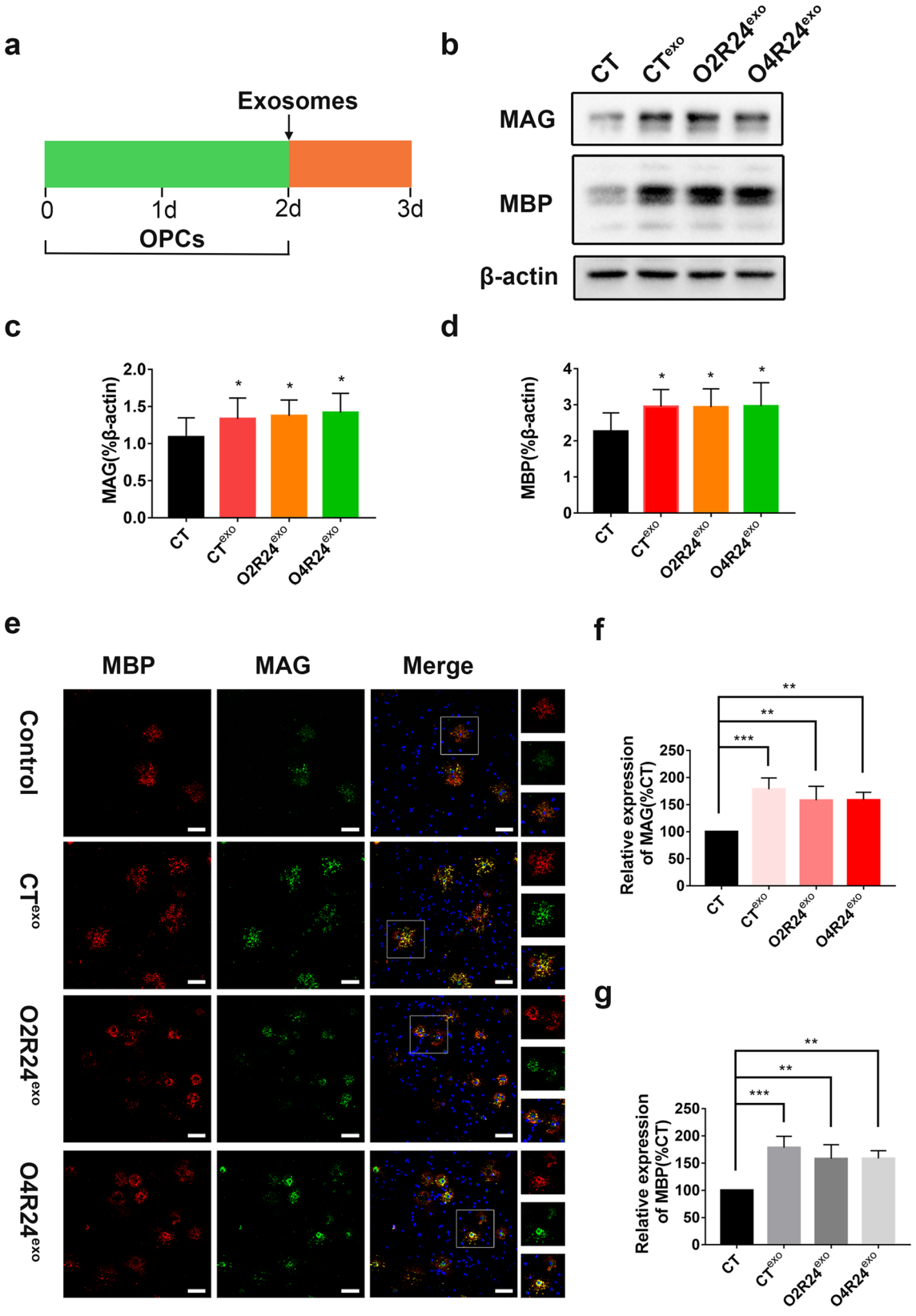
a
Exosomes
0
1d
2d
3d
OPCs
b
CT
CTexo
O2R24exo
O4R24exo
MAG
MBP
β-actin
c
MAG(%β-actin)
d
MBP(%β-actin)
e
MBP
MAG
Merge
Control
CTexo
O2R24exo
O4R24exo
f
Relative expression of MAG(%CT)
g
Relative expression of MBP(%CT)

◂**Fig. 4** AS-Exo promote the differentiation of OPCs. **a** Schematic diagram of the co-culture process of OPCs and AS-Exo in differentiation. **b** Images of western blot for MBP, MAG and β-actin in four groups. **c** Quantitative analysis of MAG in OPCs groups after control and AS-Exo (CT^{exo}, $O2R24^{exo}$, $O4R24^{exo}$) treatment. The expression of MAG was normalized to β-actin. **d** Quantitative analysis of MBP in four groups. The expression of MBP was normalized to β-actin. **e** Immunostaining images of MBP and MAG in four groups. Scale bar = 100 μm. **f** The relative expression of the ratio of the number of MAG positive to the $DAPI^+$ cells in control and AS-Exo (CT^{exo}, $O2R24^{exo}$, $O4R24^{exo}$) treatment groups. **g** The relative expression of the ratio of the number of MBP and DAPI double positive to the $DAPI^+$ cells in control and AS-Exo (CT^{exo}, $O2R24^{exo}$, $O4R24^{exo}$) treatment groups. Data are presented as mean ± SD (n = 4)

in $O2R24^{exo}$ showed no significant changes compared to control and CT^{exo}. Meanwhile, there is no significant statistical difference between control and CT^{exo} (Fig. 3b and c).

The PDGFR-α level was examined by western blot in the groups treated with PBS, CT^{exo}, $O2R24^{exo}$, $O4R24^{exo}$. In agreement with the results of EdU immunofluorescent staining, the $O4R24^{exo}$ group showed a lower level of PDGFR-α compared to control and CT^{exo} (Fig. 3d and e). In conclusion, AS-Exo with severe hypoxia can inhibit the proliferation of OPCs, but have marginal effect on OPCs' proliferation with control and mild hypoxia.

Astrocyte-derived exosomes promote the differentiation of OPCs

OPCs were cultured in proliferation medium for 2 days, then cells were washed twice with PBS and replaced with differentiation medium containing exosomes (CT^{exo}, $O2R24^{exo}$, $O4R24^{exo}$, 20 μg/ml) or PBS of the same volume as control, and the intervention lasted 24 h (Fig. 4a). Myelin basic protein (MBP) and myelin-associated glycoprotein (MAG) are specific markers of mature oligodendrocytes. The effects of exosomes on differentiation were assessed by exposing cultured OPCs to the different types of exosomes for 24 h. As shown in Fig. 4b, the expression of MBP and MAG were upregulated with CT^{exo}, $O2R24^{exo}$ and $O4R24^{exo}$ compared to control. And quantitative analysis also showed that the expression of MAG and MBP was significantly increased with AS-Exo (Fig. 4c and d), indicated that exosomes promoted differentiation.

To further confirm the effect of AS-Exo on OPCs differentiation, we monitored OPCs differentiation by double-staining with antibodies against MBP and MAG (Fig. 4e). During the preliminary experiment, it was found that the amount of apoptosis after the intervention of exosomes in different groups was rare (Fig. S2). The results of immunofluorescence staining confirmed that AS-Exo had higher numbers of MBP and MAG positive cells than control, and there is no statistical difference among CT^{exo}, $O2R24^{exo}$ and $O4R24^{exo}$ (Fig. 4e–g). Taken together, AS-Exo can promote the differentiation of OPCs in both normal and OGD conditions.

Astrocyte-derived exosomes augment the migration of OPCs in vitro

Transwell migration assay was used to detect the chemotactic movements of OPCs after AS-Exo treatment (Fig. 5a). The results showed that the number of OPCs migrated to the bottom of chamber was significantly increased with CT^{exo}, $O2R24^{exo}$, and $O4R24^{exo}$ treatment compared to negative control (Fig. 5b). In negative control, there is marginal OPCs migration. However, in the groups of exosomes, the numbers of OPCs migration increased significantly (Fig. 5b and c). In conclusion, it indicates that AS-Exo can improve chemotaxis for OPCs.

Discussion

Hypoxic-ischemic injury induces oligodendrocyte and axonal damage by releasing inflammatory factors, ROS, and excitatory amino acids [20]. The adult brain has endogenous myelin regeneration protection mechanism by activating OPCs to increase the amount of mature OLs [21, 22]. However, it was found that OPCs located in SVZ can migrate to the periphery of ischemia, but could not successfully mature and differentiate into oligodendrocytes [23, 24]. So, the proliferation and successful differentiation of OPCs into mature oligodendrocytes is a key factor in the recovery of white matter injury and demyelinating diseases [25]. Astrocytes regulate OPC's proliferation and differentiation by providing energy [26, 27], secreting cytokines [3], and exchanging materials through gap junction channels [28–30]. In this study, we demonstrated that oxygen-glucose deprivation induces the activation of astrocytes, and exosomes-derived from astrocytes under hypoxia condition can inhibit the proliferation whereas promote OPCs differentiation and migration in vitro.

The communication between exosomes and oligodendrocyte lineage cells is significant for remyelination. The exosomes produced by dendritic cells stimulated with low levels of IFNγ can promote myelination, reduce oxidative stress and improve myelination, and IFNγ-DC-Exos is preferentially taken up by oligodendrocytes [31]. MSC-exosomes increase vessel density and myelin-positive area in the striatum, improve functional recovery and white matter remodeling in rats after ICH [32]. And MSC-derived exosomes enriched in miR-17-92 improve axonal extension and myelination by regulating the PI3K/Akt/mTOR pathway to promote the recovery of function after stroke [33]. Environmental enrichment (EE) serum exosomes are enriched in miR-219, which is necessary

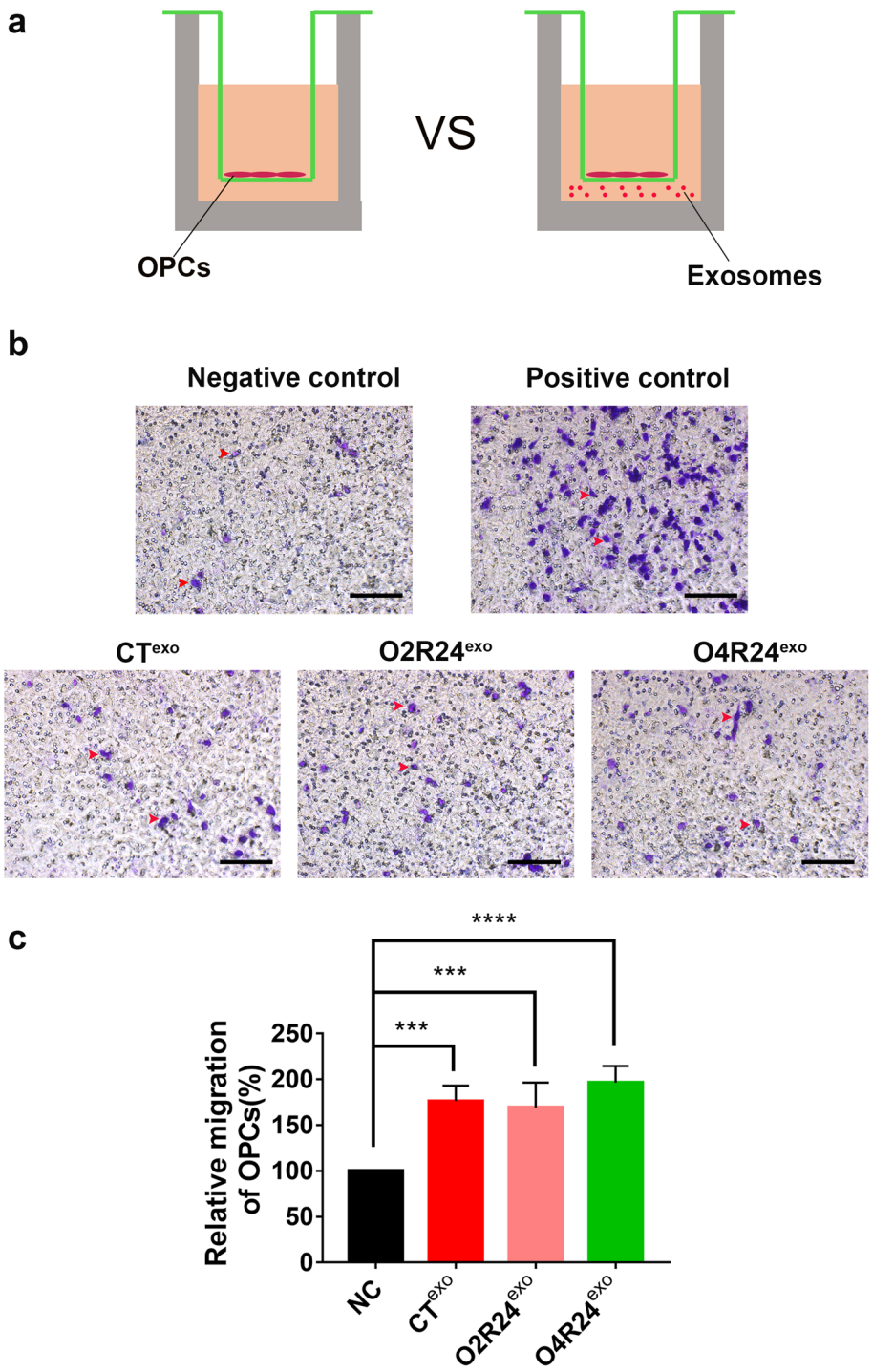

Fig. 5 AS-Exo increase the migration of OPCs in vitro. **a** A schematic diagram of the transwell test. Exosomes were added in the lower chamber to detect their chemotaxis. **b** Representative image of crystal violet staining in different groups. The lower chamber was filled with DMEM/F12 (negative control), proliferation medium (positive control), CT^{exo}, $O2R24^{exo}$, $O4R24^{exo}$. Scale bar = 100 μm. **c** Statistical results showed that all AS-Exo treatment groups could promote the migration of OPCs. Relative migration of OPCs was normalized to negative control group. *p < 0.05; **p < 0.01; ***p < 0.001; ****p < 0.0001 (n = 4)

and sufficient for OPCs differentiation into myelinating cells, and increase myelin content [34, 35]. It is reported that serum exosomes suppress T cell activation, improve the maturation of OPCs, and pregnancy exosomes facilitate OPCs migration into active CNS lesions [36]. Thus, exosomes may play a significant role in regulating the differentiation of OPCs in white matter injury. Indeed, we found that AS-Exo promoted the migration and differentiation of OPCs, and inhibit the proliferation of OPCs under severe hypoxia condition.

Recent studies have revealed that AS-Exo play an important role in functional recovery in neurological disease. The extracellular vesicles of astrocytes contain functional glutamate transporters and may regulate brain homeostasis [37]. Overproduction of phosphorylated Tau in human astrocytes exposed to amyloid beta and over-release in exosomes also

indicate the role of AS-Exo in the pathological progression of AD disease [38]. Meanwhile, AS-Exo may play an active role involving inflammation in multiple sclerosis [39], and ameliorate neuronal damage by suppressing autophagy in ischemic stroke [11]. Our results also showed that AS-Exo promoted the differentiation of oligodendrocyte precursor cells into mature oligodendrocytes, suggesting a potential role of AS-Exo in remyelination after CNS disorders.

In conclusion, our results indicate that AS-Exo can improve the differentiation and maturation of OPCs, and facilitate OPCs migration. AS-Exo under severe hypoxia significantly inhibit the proliferation of OPCs. AS-Exo may be a potential therapeutic way for myelin regeneration and repair in white matter injury or other demyelinating related diseases.

Supplementary Information The online version contains supplementary material available at https://doi.org/10.1007/s11033-021-06557-w.

Acknowledgements We thank Dr. Fengfei Ding for helpful discussion.

Author contributions MX conceived the study and designed experiments. YX, YT, YW performed the experiments and wrote the manuscript. YX, GS, QW, LX and WW analyzed the results. All authors read and approved the final version of the manuscript.

Funding The study was supported by the National Natural Science Foundation of China (81974180, 81571113). The Innovative Scientific Research foundation of HUST (2017KFYXJJ097).

Data availability The datasets used and analyzed during the current study are included in the manuscript submission.

Declarations

Conflict of interest The authors declare that they have no competing interests.

Ethical approval Animal protocols were approved by the Institutional Animal Care and Use Committee at Tongji Medical College, Huazhong University of Science and Technology.

References

1. Fern RF, Matute C, Stys PK (2014) White matter injury: ischemic and nonischemic. Glia 62:1780–1789. https://doi.org/10.1002/glia.22722
2. Miyamoto N, Maki T, Pham LD, Hayakawa K, Seo JH, Mandeville ET, Mandeville JB, Kim KW, Lo EH, Arai K (2013) Oxidative stress interferes with white matter renewal after prolonged cerebral hypoperfusion in mice. Stroke 44:3516–3521. https://doi.org/10.1161/STROKEAHA.113.002813
3. Kiray H, Lindsay SL, Hosseinzadeh S, Barnett SC (2016) The multifaceted role of astrocytes in regulating myelination. Exp Neurol 283:541–549. https://doi.org/10.1016/j.expneurol.2016.03.009
4. Lundgaard I, Osorio MJ, Kress BT, Sanggaard S, Nedergaard M (2014) White matter astrocytes in health and disease. Neuroscience 276:161–173. https://doi.org/10.1016/j.neuroscience.2013.10.050
5. Wang Q, Wang Z, Tian Y, Zhang H, Fang Y, Yu Z, Wang W, Xie M, Ding F (2018) Inhibition of astrocyte Connexin 43 channels facilitates the differentiation of oligodendrocyte precursor cells under hypoxic conditions in vitro. J Mol Neurosci 64:591–600. https://doi.org/10.1007/s12031-018-1061-y
6. Kalluri R, LeBleu VS (2020) The biology, function, and biomedical applications of exosomes. Science. https://doi.org/10.1126/science.aau6977
7. Chen JL, Chopp M (2018) Exosome therapy for stroke. Stroke 49:1083–1090. https://doi.org/10.1161/Strokeaha.117.018292
8. Riazifar M, Pone EJ, Lotvall J, Zhao W (2017) Stem cell extracellular vesicles: extended messages of regeneration. Annu Rev Pharmacol Toxicol 57:125–154. https://doi.org/10.1146/annurev-pharmtox-061616-030146
9. Li H, Luo Y, Zhu L, Hua W, Zhang Y, Zhang H, Zhang L, Li Z, Xing P, Zhang Y, Hong B, Yang P, Liu J (2019) Glia-derived exosomes: promising therapeutic targets. Life Sci 239:116951. https://doi.org/10.1016/j.lfs.2019.116951
10. Zhang ZG, Buller B, Chopp M (2019) Exosomes—beyond stem cells for restorative therapy in stroke and neurological injury. Nat Rev Neurol 15:193–203. https://doi.org/10.1038/s41582-018-0126-4
11. Pei X, Li Y, Zhu L, Zhou Z (2019) Astrocyte-derived exosomes suppress autophagy and ameliorate neuronal damage in experimental ischemic stroke. Exp Cell Res 382:111474. https://doi.org/10.1016/j.yexcr.2019.06.019
12. Pei X, Li Y, Zhu L, Zhou Z (2020) Astrocyte-derived exosomes transfer miR-190b to inhibit oxygen and glucose deprivation-induced autophagy and neuronal apoptosis. Cell Cycle 19:906–917. https://doi.org/10.1080/15384101.2020.1731649
13. Sollvander S, Nikitidou E, Brolin R, Soderberg L, Sehlin D, Lannfelt L, Erlandsson A (2016) Accumulation of amyloid-beta by astrocytes result in enlarged endosomes and microvesicle-induced apoptosis of neurons. Mol Neurodegener 11:38. https://doi.org/10.1186/s13024-016-0098-z
14. Chen Y, Xia K, Chen L, Fan D (2019) Increased interleukin-6 levels in the astrocyte-derived exosomes of sporadic amyotrophic lateral sclerosis patients. Front Neurosci 13:574. https://doi.org/10.3389/fnins.2019.00574
15. Shiow LR, Favrais G, Schirmer L, Schang AL, Cipriani S, Andres C, Wright JN, Nobuta H, Fleiss B, Gressens P, Rowitch DH (2017) Reactive astrocyte COX2-PGE2 production inhibits oligodendrocyte maturation in neonatal white matter injury. Glia 65:2024–2037. https://doi.org/10.1002/glia.23212
16. Wang R, Zhang X, Zhang J, Fan Y, Shen Y, Hu W, Chen Z (2012) Oxygen-glucose deprivation induced glial scar-like change in astrocytes. PLoS ONE 7:e37574. https://doi.org/10.1371/journal.pone.0037574
17. Miyamoto N, Maki T, Shindo A, Liang AC, Maeda M, Egawa N, Itoh K, Lo EK, Lok J, Ihara M, Arai K (2015) Astrocytes promote oligodendrogenesis after white matter damage via brain-derived neurotrophic factor. J Neurosci 35:14002–14008. https://doi.org/10.1523/JNEUROSCI.1592-15.2015
18. Lombardi M, Parolisi R, Scaroni F, Bonfanti E, Gualerzi A, Gabrielli M, Kerlero de Rosbo N, Uccelli A, Giussani P, Viani P, Garlanda C, Abbracchio MP, Chaabane L, Buffo A, Fumagalli M, Verderio C (2019) Detrimental and protective action of microglial extracellular vesicles on myelin lesions: astrocyte involvement in remyelination failure. Acta Neuropathol. https://doi.org/10.1007/s00401-019-02049-1
19. Coppi E, Maraula G, Fumagalli M, Failli P, Cellai L, Bonfanti E, Mazzoni L, Coppini R, Abbracchio MP, Pedata F, Pugliese AM (2013) UDP-glucose enhances outward K(+) currents necessary for cell differentiation and stimulates cell migration by activating

the GPR17 receptor in oligodendrocyte precursors. Glia 61:1155–1171. https://doi.org/10.1002/glia.22506
20. Shi H, Hu X, Leak RK, Shi Y, An C, Suenaga J, Chen J, Gao Y (2015) Demyelination as a rational therapeutic target for ischemic or traumatic brain injury. Exp Neurol 272:17–25. https://doi.org/10.1016/j.expneurol.2015.03.017
21. Koo E, Sheldon RA, Lee BS, Vexler ZS, Ferriero DM (2017) Effects of therapeutic hypothermia on white matter injury from murine neonatal hypoxia-ischemia. Pediatr Res 82:518–526. https://doi.org/10.1038/pr.2017.75
22. Rowitch DH, Kriegstein AR (2010) Developmental genetics of vertebrate glial-cell specification. Nature 468:214–222. https://doi.org/10.1038/nature09611
23. Xiong M, Li J, Ma SM, Yang Y, Zhou WH (2013) Effects of hypothermia on oligodendrocyte precursor cell proliferation, differentiation and maturation following hypoxia ischemia in vivo and in vitro. Exp Neurol 247:720–729. https://doi.org/10.1016/j.expneurol.2013.03.015
24. Wu X, Qu X, Zhang Q, Dong F, Yu H, Yan C, Qi D, Wang M, Liu X, Yao R (2014) Quercetin promotes proliferation and differentiation of oligodendrocyte precursor cells after oxygen/glucose deprivation-induced injury. Cell Mol Neurobiol 34:463–471. https://doi.org/10.1007/s10571-014-0030-4
25. Patel JR, McCandless EE, Dorsey D, Klein RS (2010) CXCR4 promotes differentiation of oligodendrocyte progenitors and remyelination. Proc Natl Acad Sci USA 107:11062–11067. https://doi.org/10.1073/pnas.1006301107
26. Tekkok SB, Brown AM, Westenbroek R, Pellerin L, Ransom BR (2005) Transfer of glycogen-derived lactate from astrocytes to axons via specific monocarboxylate transporters supports mouse optic nerve activity. J Neurosci Res 81:644–652. https://doi.org/10.1002/jnr.20573
27. Berghoff SA, Gerndt N, Winchenbach J, Stumpf SK, Hosang L, Odoardi F, Ruhwedel T, Bohler C, Barrette B, Stassart R, Liebetanz D, Dibaj P, Mobius W, Edgar JM, Saher G (2017) Dietary cholesterol promotes repair of demyelinated lesions in the adult brain. Nat Commun 8:14241. https://doi.org/10.1038/ncomms14241
28. Li T, Giaume C, Xiao L (2014) Connexins-mediated glia networking impacts myelination and remyelination in the central nervous system. Mol Neurobiol 49:1460–1471. https://doi.org/10.1007/s12035-013-8625-1
29. Niu J, Li T, Yi C, Huang N, Koulakoff A, Weng C, Li C, Zhao CJ, Giaume C, Xiao L (2016) Connexin-based channels contribute to metabolic pathways in the oligodendroglial lineage. J Cell Sci 129:1902–1914. https://doi.org/10.1242/jcs.178731
30. Fasciani I, Pluta P, Gonzalez-Nieto D, Martinez-Montero P, Molano J, Paino CL, Millet O, Barrio LC (2018) Directional coupling of oligodendrocyte connexin-47 and astrocyte connexin-43 gap junctions. Glia 66:2340–2352. https://doi.org/10.1002/glia.23471
31. Pusic AD, Pusic KM, Clayton BL, Kraig RP (2014) IFNgamma-stimulated dendritic cell exosomes as a potential therapeutic for remyelination. J Neuroimmunol 266:12–23. https://doi.org/10.1016/j.jneuroim.2013.10.014
32. Han Y, Seyfried D, Meng Y, Yang D, Schultz L, Chopp M, Seyfried D (2018) Multipotent mesenchymal stromal cell-derived exosomes improve functional recovery after experimental intracerebral hemorrhage in the rat. J Neurosurg. https://doi.org/10.3171/2018.2.JNS171475
33. Xin H, Liu Z, Buller B, Li Y, Golembieski W, Gan X, Wang F, Lu M, Ali MM, Zhang ZG, Chopp M (2020) MiR-17-92 enriched exosomes derived from multipotent mesenchymal stromal cells enhance axon-myelin remodeling and motor electrophysiological recovery after stroke. J Cereb Blood Flow Metab. https://doi.org/10.1177/0271678X20950489
34. Pusic KM, Pusic AD, Kraig RP (2016) Environmental enrichment stimulates immune cell secretion of exosomes that promote CNS myelination and may regulate inflammation. Cell Mol Neurobiol 36:313–325. https://doi.org/10.1007/s10571-015-0269-4
35. Pusic AD, Kraig RP (2014) Youth and environmental enrichment generate serum exosomes containing miR-219 that promote CNS myelination. Glia 62:284–299. https://doi.org/10.1002/glia.22606
36. Williams JL, Gatson NN, Smith KM, Almad A, McTigue DM, Whitacre CC (2013) Serum exosomes in pregnancy-associated immune modulation and neuroprotection during CNS autoimmunity. Clin Immunol 149:236–243. https://doi.org/10.1016/j.clim.2013.04.005
37. Gosselin RD, Meylan P, Decosterd I (2013) Extracellular microvesicles from astrocytes contain functional glutamate transporters: regulation by protein kinase C and cell activation. Front Cell Neurosci 7:251. https://doi.org/10.3389/fncel.2013.00251
38. Chiarini A, Armato U, Gardenal E, Gui L, Dal Pra I (2017) Amyloid beta-exposed human astrocytes overproduce phospho-tau and overrelease it within exosomes, effects suppressed by calcilytic NPS 2143-further implications for Alzheimer's therapy. Front Neurosci 11:217. https://doi.org/10.3389/fnins.2017.00217
39. Willis CM, Menoret A, Jellison ER, Nicaise AM, Vella AT, Crocker SJ (2017) A refined bead-free method to identify astrocytic exosomes in primary glial cultures and blood plasma. Front Neurosci 11:335. https://doi.org/10.3389/fnins.2017.00335